Proceedings World Geothermal Congress 2020+1
Reykjavik, Iceland, April - October 2021

Interdisciplinary Research for a Geothermal Carbonate Reservoir

Hermann Buness[1], Hartwig von Hartmann[1], Jennifer Ziesch[1,2], Britta Wawerzinek[1,3], Ernesto Meneses Rioseco[1], Ruediger Thomas[1]

[1] Leibniz Institute for Applied Geosciences, Stilleweg 2, 30655 Hannover

[2] now at State Authority for Mining, Energy and Geology (LBEG), Stilleweg 2, 30655 Hannover

[3] now at Helmholz Center Potsdam (GFZ), Telegrafenberg, D-14473 Potsdam

hermann.buness@leibniz-liag.de

Keywords: carbonate reservoir, 3D-seismic cube, seismic classification, seismic sequence stratigraphy, retro-deformation, s-waves, dolomitization, TH-modelling, multi-well pattern

ABSTRACT

The Upper Jurassic carbonate platform in the Bavarian Molasse Basin will be extensively used to provide the district heating system of Munich with geothermal energy. We take an interdisciplinary approach to examine a large 3D-seismic volume, without well information. The project GeoParaMoL is part of the GRAME project coordinated by the Stadtwerke München (SMW). Seismic facies analysis reveals the distribution of different carbonate rocks by analysing seismic reflection patterns. We divided the 600 m thick platform vertically; in each layer, a classification based on seismic attributes was computed. On top of this, we applied seismic sequence analysis along sections through the platform to interpret the classifications. Multicomponent recordings enable to conduct a converted wave processing and give the relationship of P- to S-wave velocity ratio (v_p/v_s) for a part of the reservoir. An unexpected high v_p/v_s ratio results for the Molasse units, which has consequences for hypocentre determination of induced seismicity. Inside the reservoir, a low v_p/v_s ratio correlates with patterns derived from facies analysis. High v_p and v_s values correlate with low v_p/v_s and are interpreted as dolomitized carbonates. We analysed tectonic features by retro-deformation that predicts sub-seismic faults invisible for seismic interpretation. A surprising result regarding the most prominent fault shows the largest strain occurred not near the fault, but approximately 500 m to 1000 m south of it. We found significant strain variations along the fault strike. A combination of these methods yields a complete picture of the geothermal reservoir. A reservoir model of the GRAME region enables a coupled thermal-hydraulic (TH) simulation and volumetric analysis. To achieve this, we generated numerically stable 3D finite element grids to handle topologically complex structures and strong hydraulic gradients at sharp lateral and vertical permeability contrasts.

1. INTRODUCTION

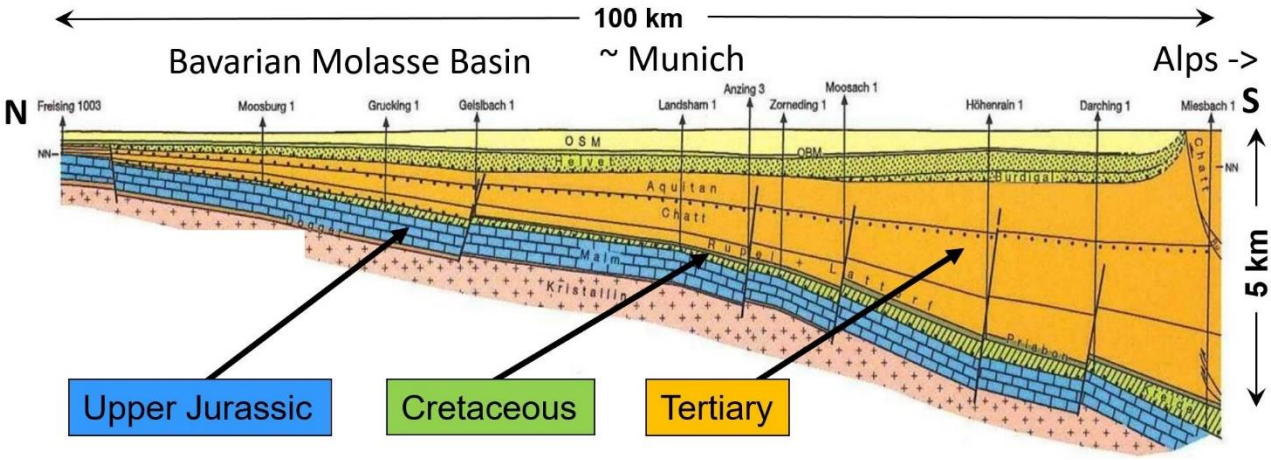

Figure 1: Simplified sketch of the geology of the Bavarian Molasse Basin (Fritzer et al. 2004). The geothermal reservoir is inside the Upper Jurassic (Malm) units, overlain by southwards increasing thick Molasse units. Beneath Munich, they reach a thickness of 2 – 3 km. Cretaceous layers thin out towards the NW in the survey area.

The Upper Jurassic (Malm) carbonate platform in the Bavarian Molasse Basin (Fig. 1) is the most utilised geothermal reservoir in Germany. Twenty-seven geothermal facilities are already in operation. Appropriate production rates are due to highly fracturing along prominent fault zones, development of karst and secondary porosity by dolomitization, especially in buildups. In the southern part of Munich, the 'Stadtwerke München' envisage a 100% supply of sustainable heat energy by the year 2040 for their district heating net. Geothermal heat shall contribute to it by an area-wide pattern of geothermal facilities (Project GRAME, Hecht and Pletl 2015).

Geothermal boreholes in the Malm have shown, that despite many successful projects, also some failures occurred (e.g. Geretsried, Mauerstetten), emphasising the need for comprehensive characterization of potential geothermal reservoirs. This is the intention of

the GeoParaMoL project (Buness et al. 2016) of the Leibniz Institute for Applied Geophysics (LIAG), that uses (1) seismic attribute analysis, (2) S-wave experiments, (3) structural analysis, including retro-deformation, and (4) thermal-hydraulic modelling to achieve this aim.

As a database for the project, a 3D-seismic survey was acquired that covers 170 km² of the southern part of Munich (Fig. 2). The survey was carried out 2016/17; the processing included CRS (common reflection surface) processing and pre-stack depth migration. This processing yielded the best image and was subsequently used for interpretation. Actually, four wells have been drilled in the survey area. 2D profiles were shot to connect boreholes in the surrounding area for depthing. Shear wave measurements were also conducted during the regular 3D-seismic survey (s. Fig. 2). In a passive experiment, the survey was additionally recorded on single, 3-component (3C), digital receivers. In this way, another 3D P-wave, as well as a 3D S-wave dataset, were acquired. In the active shear-wave experiment, the SHOVER technique (Edelmann 1981) was applied to excite shear waves directly using standard vertical vibrators.

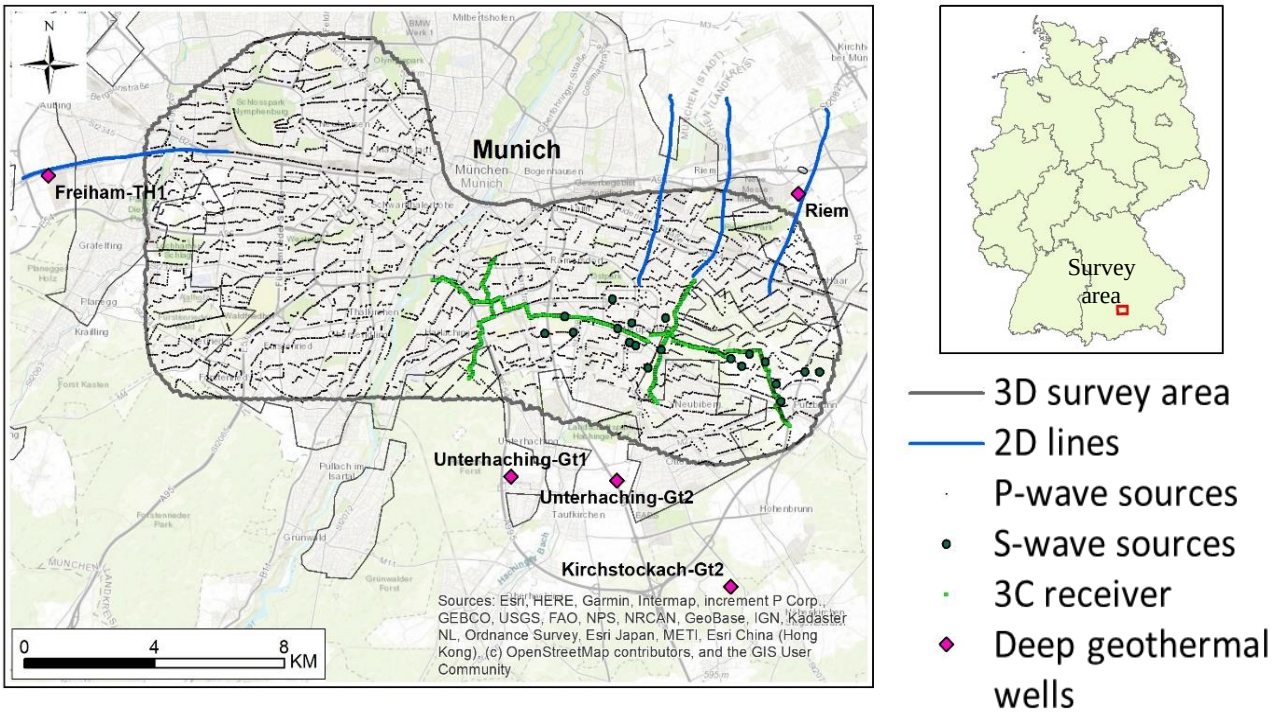

Figure 2: 3D-seismic survey covering the southern and western part of Munich and surrounding geothermal wells.

2. STRUCTURAL ANALYSIS

Faults are one of the main characteristics of geothermal reservoirs in this area, because of their role in increasing hydraulic permeability. Fault strike and dip, fault shape, faults throws and interconnections are information that helps to analyse of this impact on permeability enhancement. We analysed seven stratigraphic horizons; figure 3 shows four of them with the most prominent faults.

The survey area is characterised mainly by normal faulting. The largest of these faults is the Munich fault, showing a maximum throw up to 350 m. To the east, this fault splits into several branches and terminates. In the SE part of the area, we find another complex fault system that constitutes the continuation of faults from another 3D-seismic survey. Notably relay-ramps, hook structures and horst and graben structures can be seen. In both parts, small antithetic and synthetic faults with very small throws (<80 m) form part of a horsetail splay, typical for strike-slip regimes (Kim et al. 2004).

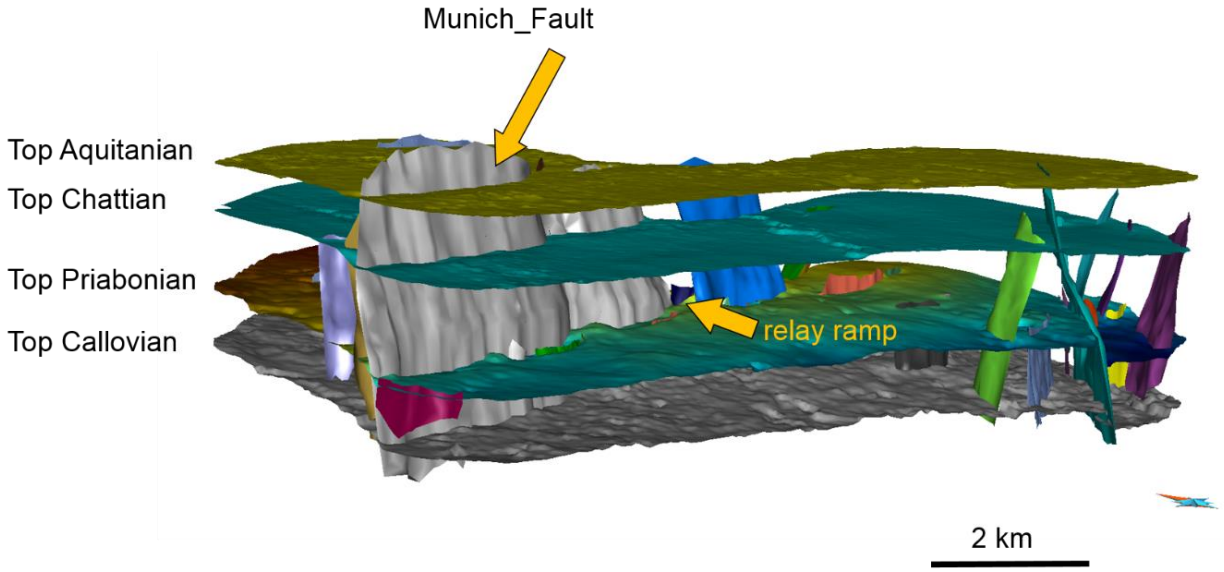

Figure 3: A 3D geological model developed from the 3D survey showing four of seven stratigraphic horizons and all faults, 2x vertical exaggeration. Top Priabonian and top Callovian approximately bound the geothermal reservoir.

Juxtaposition maps (i.e. fault throw vs strike) allow information on the timing of the faulting to be extracted. They show the maximum throw was during Cretaceous times, i.e. between Top Purbeck and Top Priabonian. Because Cretaceous units are thin and disappear towards the NW, they do not give more detail about the timing of the event. However, fault throw decreases upwards the younger Molasse units as well as downwards to deeper layers at base Malm und Dogger. This indicates that the faults probably do not extend into the basement, which may be crucial for the interpretation of induced seismicity.

The geometry of the tiplines gives a hint to the kinematic of faults (Ziesch et al. 2017): pure normal faulting leads to elliptical tiplines. However, the vertical trend of some tiplines in the survey area indicates a mixture of normal and strike-slip faulting that is confirmed by interpretation of the seismic data. Strike-slip faulting may result in a more heterogeneous distribution of hydraulic permeability than pure normal faulting.

3. FACIES CLASSIFICATION

The facies contribute by the matrix permeability to the geothermal reservoir. This permeability is in general, much lower than the permeability caused karst processes and faulting. Nevertheless, reservoir modelling has to take this permeability into account, and therefore, the facies distribution has to be known. The facies of the carbonate platform was studied from outcropping units of the Franconian and Swabian Alp in the north (Fig. 1) and a few boreholes inside the Molasse basin. The traditional model (Meyer and Schmidt-Kaler 1989) includes the distribution of large reef complexes separated by troughs consisting of differently-layered limestones. Whereas in the north coral reefs occur, they could not be confirmed by deep boreholes in the southern part. The distribution and size of these troughs in the Munich region would seem to be highly irregular (Schulz and Thomas 2012).

For seismic facies analysis, we followed an approach that is primarily oriented on the seismic data: The Malm units were divided vertically into eight layers, each of which with an approximate thickness of 70 m. Inside every layer and for every bin, the following three seismic attributes were calculated: (1) centre frequency, (2) amplitude and (3) similarity. The range of centre frequencies and amplitudes were divided into three intervals and the similarity into two intervals. An inspection of the results yielded a strong correlation between amplitudes and similarity values, i.e. small amplitudes, show less similarity and vice versa. In this case, we designed a further division of amplitude values according to similarity. This lead to altogether 18 independent combinations (Fig. 4), that we subsequently colour coded and projected on top of each layer.

The distribution of classes reveals regions with uniform amplitudes contrasting with strong variations (s. Fig. 4). These regions can be further subdivided by different frequencies; especially regions with low amplitude values show strongly varying frequencies. The pattern can be correlated between the vertical layers, towards the upper layers amplitudes as well as amplitude differences increase. We furthermore took the local distribution in each layer to interpret sedimentation environments by stratigraphic sequence analysis.

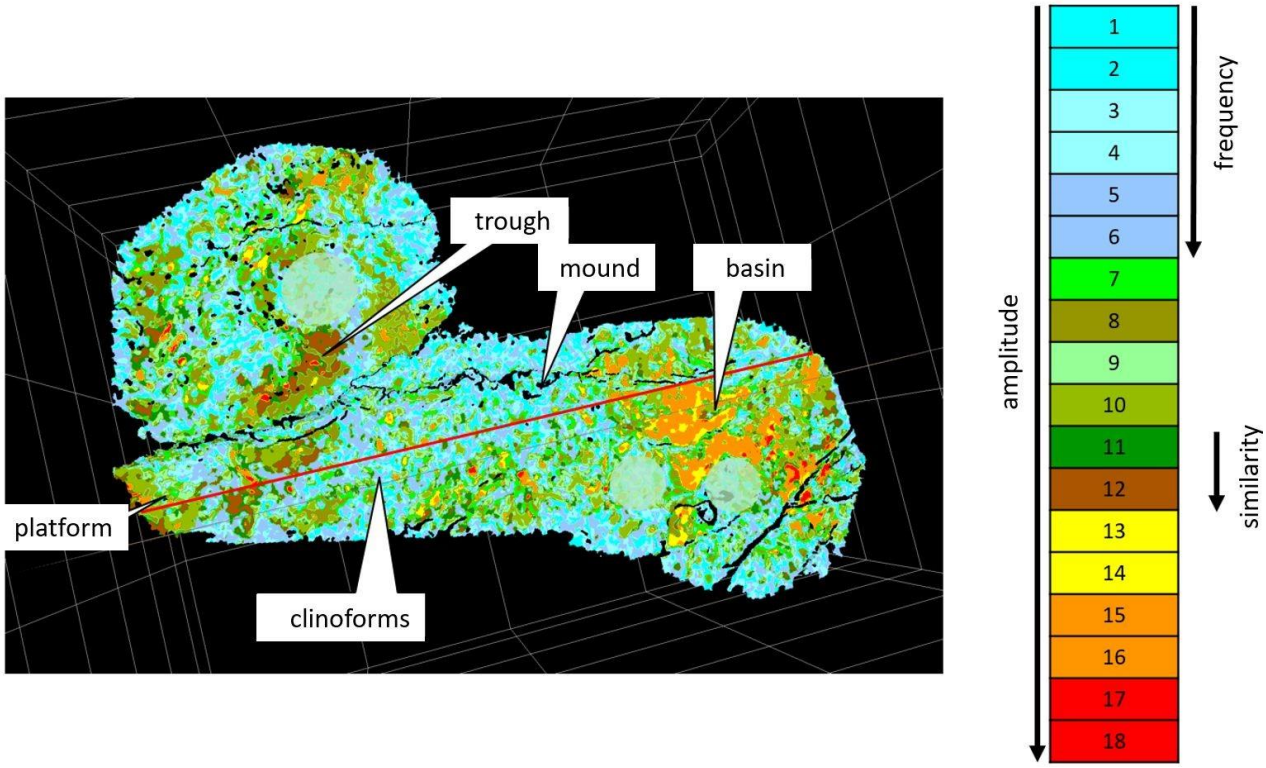

Figure 4: Attribute classes of the fifth of eight layers inside the Malm. Colour-code is shown on the right. Frequency and similarity repeat along the colour bar. The red line indicates the position of Fig. 5.

4. SEQUENCE ANALYSIS

Seismic sequence analysis helps to identify different facies by helping to reconstruct the sedimentary processes. The sequence boundary marks a timeline where sedimentary structures formed simultaneously. Strong and coherent reflections and reflection patterns help to define these boundaries. Sea level changes are the main reason for changing the sedimentary environment. They cause disruptions in the sedimentary process, which led to discontinuities in the seismic reflections. The sequence analysis is performed on seismic sections, and these interpretations were correlated with the facies maps (fig. 4). In the seismic section (fig. 5) five lateral subdivisions show different predominant seismic patterns: strong subparallel reflections, chaotic low reflective pattern, slopes and clinoforms, steep slopes and triangle structures and low reflective subparallel layering. The continuity of subparallel and inclined reflective characteristics and discontinuities at the top and bottom of clinoforms define the sequence boundaries (fig. 5, white lines). Our interpretation of the section is that on the windward and leeward side of a buildup (fig. 5, section D), different sedimentation process predominates. Section C (fig. 5) got the sedimentary infill from the buildup and an inner-platform area (section A, fig. 5). Section E (fig. 5) was drowned in the middle part and later on smaller buildup which merged into a reef complex developed.

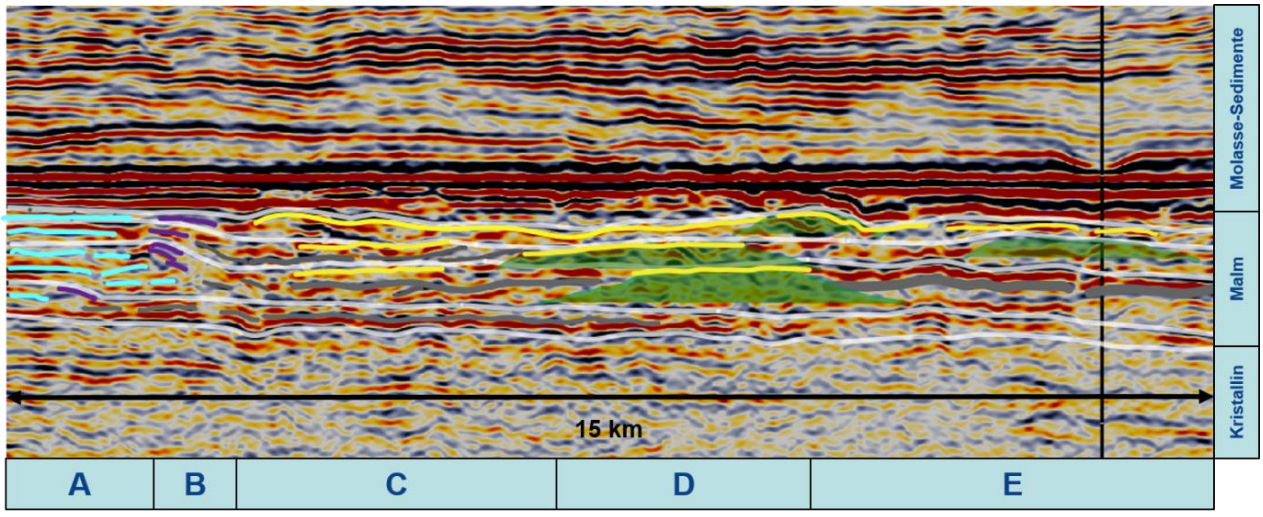

Figure 5: Facies interpretation along the section marked in fig. 4. Shown are sequence boundaries (white), mud-mounds (green), platform mud wackestones (light blue), basin mudstones (grey), shallow water grainstones (yellow) and shelf margin boundstones (purple).

The classification shown in Figure 4 represents a depth slice approximately at the top of the second layer in Figure 5 and can be thus interpreted: The low reflective region at the eastern margin corresponds to mud mounds that become apparent at the rightmost position in the section. Towards the west, a basin with very high reflectivity follows, which is cut by the section on its northern margin. Further west, a region dominated by mud mounds, characterised by lower reflectivity follows before small to medium amplitudes indicate a region were clinoforms appear. Further to the west, a trough can be correlated with medium amplitudes. The westernmost region consists of a platform showing little reflectivity. Generally, mud mounds are characterized by circular; low reflectivity structures surroundded by stronger reflectivity and by varying frequencies.

5. RETRODEFORMATION

In a first step, we cut all stratigraphic horizons into single blocks so that they could be moved independently along the fault surfaces. We calculated dip, azimuth, curvature, and cylindricity for all fault surfaces. Altogether, we created 40 blocks consisting of tetrahedra with edge lengths of 75 m.

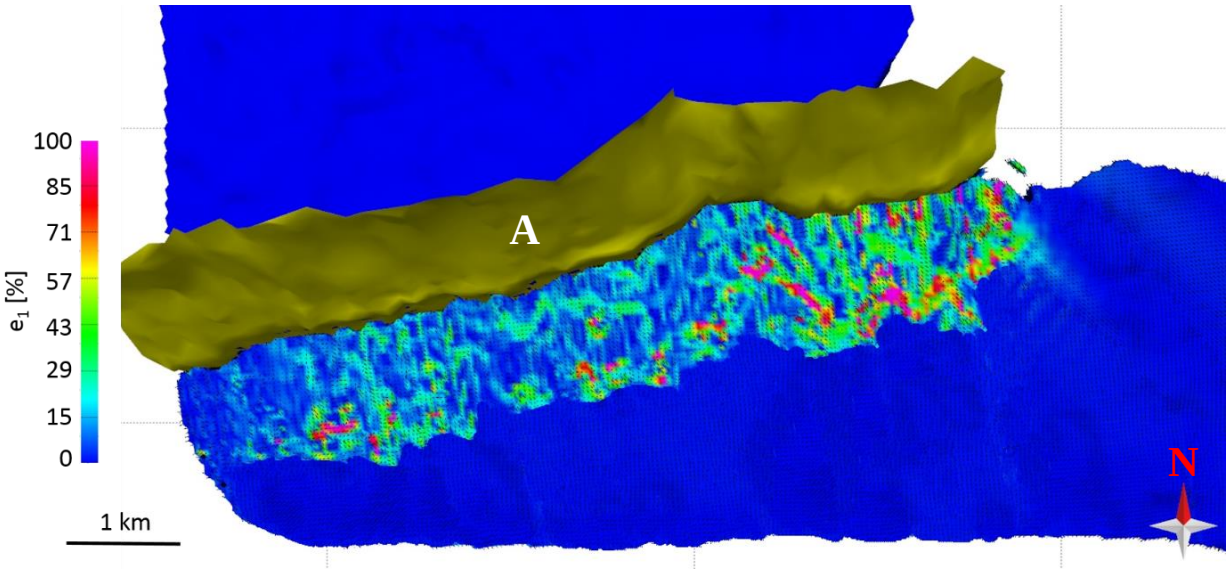

Fig. 6: Deformation at Top Purbeck (just below Top Priabonian in fig. 3) after 3D retro-deformation of all stratigraphic layers above. "A" marks the same fault as in fig. 3. Shown is the e1-magnitude, which gives a scalar quantity of the deformation of the hanging-wall. The strongest deformation is found at more than 1 km away from the fault.

The second step consists of an assignment of lithology and age of the stratigraphic layers to the volumes. An exact estimation of compaction is crucial for retro-deformation and needs data for porosity. From several databases, we calculated exponential porosity-depth functions for all Molasse sediments. Due to the lack of data, the carbonates were modelled using a constant porosity function and resulting strain values due to decompaction range between 5 % at top Aquitanian to nearly 50 % for the lower Molasse layers. They show no significant lateral variations, only near to the main faults do they decrease.

The next step comprised the retro-deformation of the hanging-wall of the largest fault: the E-W striking Munich fault with a throw of 350 m. Surprisingly, the largest values of deformation (e1-magnitude) do not appear closest to the fault, but 500 – 1000 m south of it. We can also differentiate the deformation laterally: in the western part, it is in most small with values that do not exceed 20 %, whereas in the eastern part often values of up to 85% occur. Since deformation is a proxy to the density of sub-seismic fractures, an increased amount of fractures is more probable in the eastern part, close to where the Munich fault splits into two branches. Besides the scalar value of the e1-magnitude, the deformation vectors can be derived from retro-deformation. They give the direction of maximum deformation and thus of the preferred fracture orientation. They are predominantly perpendicular to the Munich Fault. Thus we hypothesise that the Munich fault has a preferentially fault-parallel anisotropic permeability.

6. SHEAR WAVES

Shots in the eastern part of the seismic survey were recorded additionally by 3C receivers arranged on 2D lines (s. Fig. 1). After rotation of components into a radial-transversal coordinate system, we discovered that the most prominent reflections originate from the top of the carbonate platform and that the travel time relationship of the vertical to the radial component is 1.55. This would indicate a rather low VP/VS relationship. However, a 3C vertical seismic profile (VSP) from a nearby well shows a Vp/Vs relationship of more than two down to the carbonate platform and thus proves that the main energy recorded by the horizontal components results from converted waves.

Knowing the Vp/Vs relationship allows a converted wave processing of the relatively small 3C seismic volume. We could follow continuous horizons in this volume, from the top of the reservoir as well as from inside the reservoir and correlated them with reflectors from the P-wave seismic volume. The traveltimes of the corresponding reflectors could now be determined, followed by the calculation of the interval travel times between two horizons. This finally gives the Vp/Vs (Garotta 1987, Tessmer and Behle 1988).

The results show a Vp/Vs relationship with a median value of 1.92 above the carbonate platform. This is significantly higher than the values assumed so far (1.6 – 1.7; Schulz and Thomas 2012). This finding is of significance for the determination of hypocentres of

induced seismicity occurring at geothermal facilities in the surrounding area (Megies and Wassermann, 2014). The high V_P/V_S relationship hints at events at the basis of the carbonate platform and not deep inside the crystalline basement.

In the reservoir, the variation of the V_P/V_S values from 1.5 – 2.1 is larger than in the Molasse units. In Figure 7, a region of low values (1.5 – 1-8) is surrounded by high values (>1.8). This pattern is opposed to the facies classification (s. Fig. 4). Correlation is possible: low V_P/V_S values correspond to blue facies classes and high values to orange classes. Since the colour code is dominated by the seismic amplitudes, we see low V_P/V_S values where reflectivity is also low and vice versa.

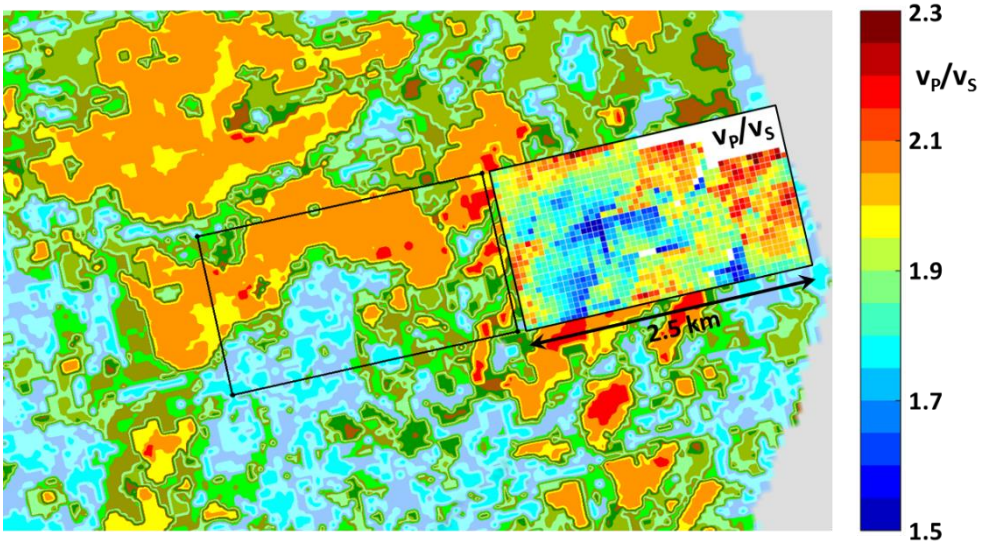

Fig. 7: Vp/Vs relationship observed from interval velocities inside the reservoir inserted in the facies classification map of Figure 4. The pattern of both independently-derived quantities correlates well.

The Vp/Vs relationship allows conclusions to be made about the lithology, facies and porosity that cannot be drawn from either Vp or Vs alone (Tatham & McCormack, 1991). The relationship allows differentiating between sandstone (1.59-1.76), dolomite (1.78-1.84) and limestone (1.84-1.99) (Domenico 1984). The relationship also varies for different facies: in a lagoon environment, lower values than in high porosity limestones have been found by Garotta (1985). Emery & Stewart (2006) show that Vp/Vs ratios increase with increasing porosity.

The Vp/Vs relationship correlates in the carbonate platform with Vp and Vs values: high velocities are connected with a low Vp/Vs relationship and vice versa. This can be correlated to the elastic properties of limestone and dolomite. The velocities in dolomite are higher than in limestone, whereas the Vp/Vs relationship is lower (Pickett 1963). The combination of an increase in Vp and Vs correlated with a decrease in the relationship is, therefore interpreted as a dolomitized region.

7. THERMAL-HYDRAULIC MODELLING

The basis for thermal-hydraulic (TH) modelling was the structural geological and the reservoir classification, as described above. However, both of them are too detailed to be used directly in a TH-modelling. A consistent reservoir architecture has to be considered for the 3D finite element (FE) net. A modelling of all geological faults is not possible, therefore we build a hierarchy of faults according to the criteria (1) faults that confine the reservoir (2) faults that separate compartments inside the reservoir (3) faults that probably influence the movement of fluid and (4) faults that could act as barriers. In order to construct a water-tight reservoir-model that is suited for dynamic simulations, we developed the following workflow: smoothing of complex surfaces, homogenisation of triangulated surfaces, removal of gaps, connection of horizon and fault surfaces and association of nodes in the cutting lines between faults and between faults and horizons. In this way, we constructed a geological-consistent, structural- and stratigraphic-unified reservoir model.

Another important aspect constitutes the near- and far-field pressure distribution that results from the constant injection and production of fluids in such geothermal doublet and triplet arrays as well as other multi-well systems such as hexagon patterns. Figure 8 shows the pressure field (hydraulic head) after 50 years of modelling time caused by a geothermal doublet array and hexagon multi-well systems, respectively. Successful optimisation of multi-well patterns in highly heterogeneous carbonate reservoirs not only depends on a fine characterisation of the reservoir but also on the complex, long-term, thermal-hydraulic interactions of the multi-well array with existing neighbouring geothermal wells already in operation. Moreover, the well spacing density plays a major role in the generated pressure far-field. Model results indicate that fluid flow regime in the entire region of greater Munich is highly controlled by such high densely-spaced doublet array. A stationary flow regime is established a couple of years after the onset of injection and production. Site-specific thermal and hydrogeological conditions make special multi-well design systems more appropriate than regular geothermal doublet arrays (Fig. 8).

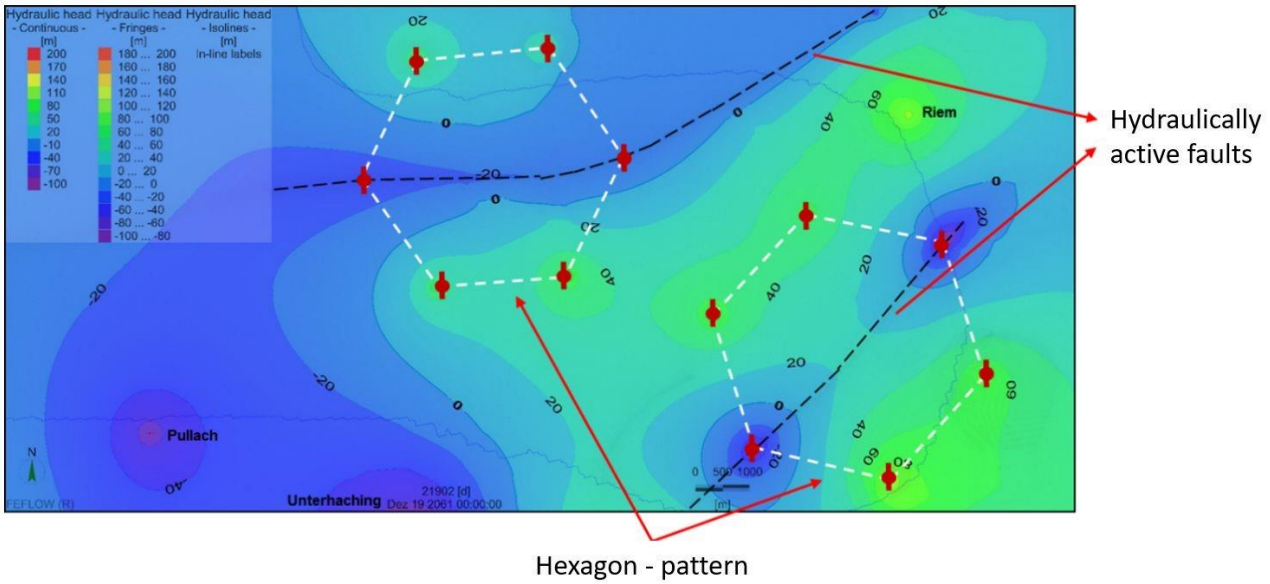

Figure 8: Pressure field (hydraulic head) in the first main influx zone for multi-well configurations (hexagon-configuration of 6 geothermal wells) after 50 years of simulation time. Red symbols display injection and production wells. Different hydraulically active faults are shown with black dashed lines. Note that production wells are placed in the fault zones while injection wells are placed around the faults. 150 l/s of thermal water are constantly produced in each production well, and 75 l/s of cooled thermal water is permanently reinjected in the injection wells.

8. CONCLUSIONS

In this project, we have applied methods that have never been used before in the geothermal exploration of the Bavarian Molasse, with promising results. We believe that the combination of seismic sequence stratigraphy and classification algorithms based on seismic attributes leads to a better understanding of the development of the carbonate platform. The database consisted of a large 170 km2 seismic dataset without well control. We aimed to understand the overall picture, in this case, the development of the carbonate platform and its overburden. This is impractical if the seismic volume is too small, as it is often the case of geothermal surveys that cover only the immediate surrounding area of a doublet. Although as in our case, the survey was quite large, it was able to allow a limited insight into the carbonate depositional processes. In a follow-up project, we will try to expand the seismic database.

The evaluation of multicomponent seismic recording hints at dolomitized regions inside the reservoir. Since the pattern of this distribution correlates with the independently derived facies classification, we are confident about its reliability. Therefore, we believe it is sensible to conduct future 3C seismic surveys using 3C receivers. During the Munich survey, we compared 3C single sensors with traditional geophone group recordings and did not notice significant differences, despite the noisy urban environment (Wawerzinek et al. 2017).

The technique of retro-deformation enables the predicttion of sub-seismic faults (Ziesch et al. 2019). This technique strongly depends on the morphology of fault zones – hence, it is crucial to invest enough effort in an accurate fault plane determination. Moreover, we were able to explain by retro-deformation some features in the structure of the Molasse sediments (i.e. rollover and drag folds), which are due to the strong variation of the fault dip above and within the carbonate platform. The prediction of sub-seismic fractures by retro-deformation looks plausible but needs control by drilling (and FMI data) when the SWM project proceeds.

We included all the findings into a reservoir model and conducted long-time thermal-hydraulic modelling. The transformation of the structural and the facies models need inevitable simplification before it is applied in such a model. Since new data will come in continuously during future exploitation, rapid updating of the reservoir model is crucial. From our modelling of the status quo knowledge, we conclude, that a multi-well design, e.g. hexagon configurations, taking site-specific conditions (e.g. faults or facies variation) into account, has significant advantages over a regular array of doublets.

ACKNOWLEDGEMENTS

We thank Stadtwerke München (SWM) for good cooperation. The project is supported financially by the Federal Ministry for Economic Affairs and Energy (FKZ 0325787B).

REFERENCES

Buness, H., von Hartmann, H., Lueschen, E., Meneses Rioseco, E., Wawerzinek, B., Ziesch, J. & Thomas, R. (2016): GeoParaMoL: Eine Integration verschiedener Methoden zur Reduzierung des Fündigkeitsrisikos in der bayrischen Molasse, Geothermische Energie, 85, 22-23.

Edelmann, H.A.K. (1981): SHOVER shear-wave generation by vibration orthogonal to the polarization. Geophysical Prospecting 29, 541-549.

Fritzer, T., Settles, E. and Dorsch, K. (2004): Bayerischer Geothermieatlas 2004. Bayerisches Staatsminsterium für Wirschaft, Energie und Technologie, München.

Garotta, R. (1985): Observation of shear waves and correlation with P events. In G. Dohr (ed.): Seismic Shear Waves, Part B: Applications, Geophysical Press.

Garotta, R. (1987): Two-component acquisition as a routine procedure. In S.H. Danbom & Domenico, S.N. (eds.): Shear Wave Exploration, Geophysical Developments Series No. 1, Society of Exploration Geophysicists.

Hecht, C. and Pletl, C.(2015): Das Verbundprojekt GRAME – Wegweiser für eine geothermische Wärmeversorgung urbaner Ballungsräume. Geothermische Energie, Heft 82, 2015/2.

Kim, Y.-S., Peacock, D.C.P. & Sanderson, D.J. (2004): Fault damage zones. Journal of Structural Geology, 26, 503-517.

Megies, T. and Wassermann, J. (2014): Microseismicity observed at a non-pressure-stimulated geothermal power plant. Geothermics 52, 36-49.

Meyer, R.K.F., Schmidt-Kaler H., 1989. Paläogeographischer Atlas des süddeutschen Oberjura (Malm), Geologisches Jahrbuch, Reihe A, Heft 115, Schweitzerbart‘sche Verlagsbuchhandlung, Stuttgart.

Pickett, G. R. (1963): Acoustic character logs and their application in formation evaluation. Journal of Petroleum Technology 15, 659-667.

Schulz, R. and Thomas, R. (2012): Geothermische Charakterisierung von karstig-klüftigen Aquiferen im Großraum München – Endbericht. LIAG Bericht, Archiv Nr. 130392, Hannover.

Tessmer, G. and Behle, A. (1988): Common reflection point data-stacking technique for converted waves. Geophysical Prospecting 36, 671-688.

Wawerzinek, B., Buness, H. & Thomas, R. (2017): Beschleunigungssensoren bei einer 3D-Seismik in München: Eine Alternative? - Tagung der Deutschen Geophysikalischen Gesellschaft, 27.-30.03.2017; Potsdam.

Ziesch, J., Aruffo, C.M., Tanner, D.C., Beilecke, T., Dance, T., Henk, A., Weber, B., Tenthorey, E., Lippmann, A. & Krawczyk, C.M. (2017): Geological structure and kinematics of normal faults in the Otway Basin, Australia, based on quantitative analysis of 3-D seismic reflection data. Basin Research, 29: 129–148. DOI:10.1111/bre.12146.

Ziesch, J., Tanner, D., Krawczyk, C. (2019): Subseismic pathway prediction by three-dimensional structural restoration and strain analysis based on seismic interpretation. AAPG Bulletin, in press (nn 2019), pp. 1–27.

Verma, A., and Pruess, K.: Enhancement of Steam Phase Relative Permeability Due to Phase Transformation Effects in Porous Media, *Proceedings*, 11th Workshop on Geothermal Reservoir Engineering, Stanford University, Stanford, CA (1986). <Reference Style>

Wang, C.T., and Horne, R.N.: Boiling Flow in a Horizontal Fracture, *Geothermics*, **29**, (1999), 759-772. <Reference Style>